



PAPER

View Article Online
View Journal | View Issue



Cite this: *Environ. Sci.: Atmos.*, 2023, 3, 760

Modeling the fate and involuntary exposure to tetrahydrocannabinol emitted from indoor cannabis smoking†

Amirashkan Askari, ^a Frank Wania ^{bc} and Arthur W. H. Chan ^{ac}

Indoor air quality implications of cannabis consumption are of increasing significance following the recent trends toward legalization in many countries. Here, a level IV fugacity model is used to predict the time-variant fate of tetrahydrocannabinol (THC) emitted from cannabis smoking in an evaluative indoor environment and the resultant involuntary exposure to THC of residents of different age. With daily smoking of a typical cannabis cigarette containing 30 mg THC over one hour per day for one year, we predict THC indoor air concentrations to fall to values less than 100 ng m⁻³ within the first months, while concentrations on a carpet and vinyl flooring can reach more than 1 mg m⁻³ within one year. Non-dietary ingestion and inhalation are identified as the main routes of involuntary exposure for infants and adult residents, respectively, with rates of THC intake for infants exceeding those for adults by two orders of magnitude. Improved ventilation and PM filtration are demonstrated to be effective measures to reduce THC exposure levels, while leaving the smoking site is partially effective for that purpose. Sensitivity analysis reveals that the model results are most sensitive to input values for airborne particulate matter (PM) levels and parameters associated with air-to-surface partitioning, suggesting that a better understanding of these parameters is needed.

Received 16th November 2022
Accepted 8th March 2023

DOI: 10.1039/d2ea00155a

rsc.li/esatmospheres

Environmental significance

Smoking is the most prevalent cannabis consumption method, and an important source of indoor air pollution. As recreational cannabis use becomes legal in more jurisdictions, involuntary exposure of indoor occupants, including infants, to psychoactive emissions from cannabis smoking is a critical issue. Indoor occupants' exposure to cannabis emissions is driven by the dynamic trends of the emitted compounds partitioning between indoor air and different surface compartments and their loss by reaction, ventilation, and cleaning. A multi-compartmental time-dependent mass transport model was employed to predict the distribution of tetrahydrocannabinol (THC) from cannabis smoking among indoor compartments and passive THC uptakes for adults and toddlers. Major exposure routes and effective mitigation strategies to reduce exposure were identified.

Introduction

Cannabis is the most widely cultivated and consumed psychoactive drug globally.¹ The United Nations Office of Drug and Crime estimated more than 190 million users worldwide in 2016, which was far higher than those for other drugs.² The general trend of cannabis legal status, especially in western countries, is a timeline of gradual decriminalization or legalization. In North America, following the legalization of non-medical cannabis in Washington and Colorado in 2013, many jurisdictions within the United States and Canada followed suit

during the subsequent years. Since the legalization of non-medical cannabis in Canada in October 2018, there has been a 22 percent increase in reported users relative to the previous 12 month cycle.³ The National Cannabis Survey in Canada indicates cannabis to be more socially acceptable and associated with less risk than tobacco and alcohol from a public point of view.⁴ Such phenomena are expected to shift cannabis consumption locations to everyday social contexts such as bars, restaurants, and residences. Posis *et al.* have identified smoking as the most common method of cannabis consumption in California, US.⁵ They also found that cannabis smoking mainly occurred in indoor spaces. Siegel indicated passive exposure of non-smoking residents to cannabis emissions as a significant concern related to indoor cannabis usage, mainly at residences.⁶ Passive exposure of infants to indoor emissions of cannabis is critical given their typical vulnerability to environmental pollution and drug emissions.⁷ An American nationwide study showed that the number of parents with children at home

^aDepartment of Chemical Engineering and Applied Chemistry, University of Toronto, Toronto, Ontario M5S 3E5, Canada. E-mail: arthurwh.chan@utoronto.ca

^bDepartment of Physical and Environmental Sciences, University of Toronto Scarborough, Toronto, Ontario M1C 1A4, Canada

^cDepartment of Chemistry, University of Toronto, Toronto, Ontario, M5S 3H6, Canada

† Electronic supplementary information (ESI) available. See DOI: <https://doi.org/10.1039/d2ea00155a>



who smoked tobacco cigarettes indoors declined from 2005 to 2012, while the number of such parents who smoked cannabis increased.⁸ These considerations make the indoor air quality implications of cannabis consumption, especially the exposure of non-users to cannabis emissions, an area of concern worthy of further research.

Various chemical species in the cannabis plant matrix lead to a diverse chemical profile for emissions associated with cannabis smoking. Among the compounds in cannabis smoking emissions, cannabinoids are terpenophenolic species that act as a ligand to cannabinoid receptors in the human nervous system and hence trigger psychotropic experiences in the cannabis user.⁹ More than ten subclasses of cannabinoids are biosynthesized in the cannabis plant, including tetrahydrocannabinol (THC), to which psychotropic effects are primarily attributed, and cannabidiol (CBD) which is the main ingredient of cannabis-derived oils.¹⁰ Aside from cannabinoids, cannabis emissions contain other chemicals like terpenoids, alkaloids, and flavonoids¹⁰ and heavy metals such as lead, cadmium, and mercury,¹¹ which can be significant in terms of air quality and human exposure.

The literature is relatively sparse regarding the occurrence of cannabis-derived species in indoor air or compartments. Chou *et al.* developed an analytical method to measure airborne THC from cannabis smoking in indoor air utilizing gas chromatography.¹² Cecinato *et al.* measured cannabinoid levels in dust samples from indoor spaces like homes and airports.¹³ As cannabis emissions become more relevant to indoor air quality issues, a modeling investigation aimed at identifying the critical media influencing passive exposure to chemicals released from cannabis smoking and the efficacy of strategies to alleviate involuntary exposure is needed. Furthermore, modeling studies yield preliminary data that can help building managers, property owners, and policymakers address indoor air quality issues related to cannabis smoking in the absence of empirical data. Recently, Yeh *et al.* used a steady-state fate and exposure modeling framework to examine indoor residents' exposure to species emitted from cannabis smoking, including THC. They identified non-dietary ingestion as the main route of exposure to indoor THC.¹⁴

While the steady-state assumption is a good first approximation, the intermittent nature of cannabis smoking in combination with THC's extremely low volatility (octanol-air equilibrium partitioning ratio K_{OA} greater than 10^{12} at room temperature, see Section S2†) makes it unlikely that a steady state is reached in indoor spaces within relevant timescales.¹⁵ Thus, there is a need to employ a time-dependent fate and exposure model to examine the dynamic behavior of THC as it partitions to different indoor compartments from air following cannabis smoking. This study employs a time-dependent indoor mass balance model to predict the fate of, and human exposure to, THC emitted from cannabis smoking. The fate analysis predicts the dynamic distribution of THC among distinct compartments of an indoor space. This characterization highlights indoor compartments acting as significant THC reservoirs and exposure intermediates. The exposure analysis predicts passive THC uptake by residents of different ages

through different routes. Furthermore, the efficacy of various mitigating strategies in reducing involuntary exposure to THC from cannabis smoking is examined. Finally, a Monte Carlo simulation investigates the impact of critical input parameters on model predictions. The insights from this study can be used in future works to prioritize sampling media for projects aiming at characterizing indoor microenvironment pollution due to cannabis smoking, implementing exposure mitigation strategies given smoking and occupancy patterns, and inspecting variability and uncertainty of critical parameters influencing passive exposure to THC from cannabis smoking.

Methods

Evaluative environment

The modeled environment was adapted from the one described in the ICECRM model by Zhang *et al.*¹⁶ The model domain is assumed to be a single room with a floor area of 25 m² and a wall height of 3 m. This assumes that a room is more likely to be well-mixed with respect to THC emissions than an entire residence. Within this domain, chemical species move between indoor air and several indoor compartments. Adopting the approach by Shin *et al.*,¹⁷ indoor air is assumed to contain $\sim 40 \mu\text{g m}^{-3}$ of suspended particles of different sizes.¹⁶ Among the indoor compartments, vinyl flooring and carpet represent bare floor and fibrous matting surfaces, respectively. Polyurethane foam (PUF) is included as a compartment to represent sponge-like articles used in furniture and upholstery, which can exchange mass with air through compression and re-expansion. The remaining indoor surfaces are assumed to be covered by a thin layer of an organic film. The comprehensive list of indoor compartments and their dimensions can be found in ESI† (Section S1).

Note that each of the compartments mentioned above (*e.g.*, carpet) may differ from one indoor space to the other in the real world. As discussed by Zhang *et al.*¹⁶ and Li *et al.*¹⁸ in more detail, the partitioning of a chemical between indoor compartments is characterized by several empirical and semi-empirical correlations developed based on observations of a limited number of species. One must be cautious with extrapolating the results of such correlations to settings different from those used to develop the correlations.

Mass balance equations

This study uses a set of time-variant (non-steady-state) mass balance equations to account for indoor fate and exposure to the THC emitted by cannabis smoking. The mass balance equation for the species of interest (*i.e.*, THC) in each compartment is given by eqn (1).

$$\frac{dm_i}{dt} = S_i + \sum_{j \neq i} (N_{ji} - N_{ij}) - R_i \quad (1)$$

In eqn (1), $\frac{dm_i}{dt}$ is the rate of change in the amount of THC in compartment *i* in moles per hour. S_i and R_i refer to rates of generation and loss of THC within compartment *i*, respectively, in moles per hour. Air is the only compartment with a non-zero



generation rate corresponding to the THC emission rate due to cannabis smoking. This study inspects the effects of one hour of cannabis smoking per day. As is discussed with more detail in Section S3.2,[†] the THC emission rate to air, S_A , is assumed to alternate periodically between zero and a non-zero value associated with THC release from a single 300 mg cannabis cigarette containing 10% THC by weight. N_{ij} and N_{ji} designate the rates of THC transfer from compartment i to compartment j and *vice versa*.

Following Li *et al.*,¹⁸ we used a level IV fugacity modeling framework to calculate the terms in eqn (1). The details of the fugacity modelling approach are discussed by Mackay.¹⁹ Briefly, in this framework, concentrations and mass transfer rates are calculated using fugacity, a thermodynamic property closely related to the chemical potential.²⁰ The number of moles in compartment i , m_i , is related to fugacity within that compartment as shown in eqn (2).

$$m_i = V_i \times \text{BZ}_i \times f_i \quad (2)$$

where V_i , BZ_i , and f_i refer to the volume in m^3 , the bulk fugacity capacity of THC in $\text{mol m}^{-3} \text{Pa}^{-1}$, and fugacity of THC in Pa, respectively for compartment i . Rates of mass transfer between compartments, N_{ij} , are quantified as products of D -values D_{ij} in $\text{mol Pa}^{-1} \text{h}^{-1}$, and the fugacity in the originating compartment i , as given in eqn (3).

$$N_{ij} = D_{ij} \times f_i \quad (3)$$

Airborne THC can be present in gas and particulate matter (PM). Therefore, THC exchange between air and the other indoor compartments occurs in parallel through particle deposition/resuspension and diffusive gas exchange. As discussed in Section S2,[†] the mass transfer between air and indoor compartments is governed by the deposition/resuspension rates of the PM and by THC's affinity for organic phases, as given by its air-to-surface partitioning ratios. The model does not account for the temporal variability in particle concentrations occurring during the cannabis smoking.²¹

THC is assumed to be lost from a surface compartment by degradation loss or through removal of THC sorbed to deposited particulate matter, *i.e.*, by dusting. The two removal processes for airborne THC are gas-phase reactions and building ventilation (see Table S4[†] for more details on calculating THC compartmental loss rates). Note that indoor oxidant levels, which control gas phase and surface reactions, and ventilation rates depend on several factors, including but not limited to outdoor climate, ambient air quality, and building design and operation. We used some typical values for oxidant levels and air exchange rates (given in Table S4[†]) that are based on data in the scientific literature. As will be discussed below, the model predictions are significantly sensitive to the values assumed for some of these parameters. Hence, we encourage future users to vary the applicable input parameters when characterizing indoor spaces with conditions different from the evaluative environment discussed here. Model outputs for alternative scenarios associated with various values of the air exchange rate, indoor chemistry, and

other impactful parameters are discussed in more detail in the following paragraphs (see Fig. 6 and Section S4[†]).

Rates of removal are again calculated as products of a D -value and the fugacity in the compartment where the loss occurs, as given in eqn (4).

$$R_i = D_{\text{removal},i} \times f_i \quad (4)$$

We used equations from Li *et al.* to calculate values of D_{ij} in eqn (3) and $D_{\text{removal},i}$ in eqn (4).¹⁸ More details about calculating the parameters in eqn (1)–(4) are given in Section S2.[†] Table S1[†] lists key thermodynamic parameters of THC used in this study as inputs to the fugacity model.

Exposure analysis

The model was run for one year (*i.e.*, 365 days), assuming the THC associated with the side-stream smoke of a single cannabis cigarette, as described by Berthet *et al.*,²² is emitted into the indoor air for one hour daily. We assume the THC present in the main-stream smoke is almost entirely absorbed into the drug user's body, and there is therefore no THC in the smoker's exhaled breath.

In this study we estimate the exposure of an adult and a toddler, who are distinguished based on body size (80 kg and 12 kg, respectively) and the frequency of hygienic activities (see Tables S6 and S7[†]). We added the mass balance equations associated with passive exposure to THC for a single indoor occupant, either adult or toddler, to the mass balance equations set to examine involuntary THC uptake (see Table S5[†]). Modeling scenarios involving the presence of more than one person are beyond the scope of this work. The passive indoor resident was assumed to be exposed to THC from cannabis smoking through three routes of exposure, including inhalation, non-dietary ingestion, and dermal permeation. This study does not consider involuntary exposure to THC due to ingesting food or drink contaminated with THC from cannabis smoking. Following the approach by Zhang *et al.*,¹⁶ the passive resident was represented by three compartments including hands, remainder of skin, and body interior within the fugacity modeling framework (see Table S5[†]). Eqn (5) shows the rate of exposure to THC (*i.e.*, the THC uptake rate) in mol h^{-1} through the three routes of exposure mentioned above.

$$N_{\text{exposure}} = N_{\text{AB}}\phi_{\text{inh}} + (N_{\text{fuM}} + N_{\text{HM}})\phi_{\text{ing}} + (N_{\text{H,dermal}} + N_{\text{S,dermal}})\phi_{\text{derm}} \quad (5)$$

In eqn (5), N_{AB} is the rate of mass transfer from air to body through inhalation. N_{fuM} and N_{HM} are THC mass transfer rates associated with putting objects (approximated as upward-facing organic films) and hands into one's mouth, respectively. As discussed in Section S3.1,[†] putting objects into one's mouth is assumed to happen only for toddlers. $N_{\text{H,dermal}}$ and $N_{\text{S,dermal}}$ refer to THC mass transfer rates by dermal permeation through hands' skin and the remainder of one's skin, respectively. The THC accumulated on one's hand could originate from the air or from touching indoor surfaces. Only a fraction of the THC introduced to the body is absorbed depending on a compound's



bioavailability. ϕ_{inh} , ϕ_{ing} , and ϕ_{derm} refer to THC's bioavailability values associated with inhalation, non-dietary ingestion, and dermal permeation, respectively. More details about the terms included in eqn (5) are discussed in Sections S3.1 and S3.3.†

The average of the body mass-normalized intake rate, Exp_{avg} in $\mu\text{g day}^{-1} \text{kg}^{-1}$, is given by eqn (6).

$$\text{Exp}_{\text{avg}} = \frac{10^6 \mu\text{g g}^{-1} \times \text{MW}_{\text{THC}}}{\frac{1 \text{ day}}{24 \text{ hour}} \times W \times (t_f - t_i)} \times \int_{t_i}^{t_f} N_{\text{exposure}}(t') dt' \quad (6)$$

In eqn (6), the uptake rate, as given by eqn (5), is integrated over the time interval from t_i to t_f . MW_{THC} is THC's molecular weight (314.47 g mol⁻¹), and W is the resident's body weight in kilograms.

Exposure mitigation strategies

We assessed the efficacy of some common strategies to combat indoor air pollution for reducing involuntary exposure to THC from smoking. As will be discussed below, airborne PM is the primary vehicle for THC transport to indoor surfaces. Thus, any mitigation strategy that reduces airborne PM, such as enhanced ventilation and PM removal with filters, may be effective in reducing passive exposure to indoor THC. These measures are most effective if deployed during smoking, when THC concentrations in air are highest (see Fig. 2). However, since cannabis users may feel uncomfortable with ventilation or PM removal (e.g., noise from a PM-removing air cleaner), mitigation measures may not be practical during this time. Thus, we also consider cases of implementing PM-reducing measures for one hour after smoking.

Leaving the indoor space for a THC-free environment is another feasible strategy to reduce exposure to cannabis emissions. Indoor residents are assumed to be exposed to a THC-free environment during their absence period, where THC can still be depleted from their bodies through continued metabolism and elimination.

Surface cleaning is another possible strategy to reduce passive exposure to THC from indoor cannabis smoking. Upward-facing organic films are touched by both adults and toddlers more frequently compared to other indoor surfaces (see Table S7†). Furthermore, as discussed earlier, mouthing objects covered by organic films is a major driver for toddlers' exposure to THC through non-dietary ingestion. Therefore, we test the effectiveness of cleaning upward-facing organic films to reduce involuntary exposure to indoor THC. Because our default model settings already involve regular dusting, i.e., removing PM accumulated on surfaces (see Table S4†), the extra cleaning considered here involves measures other than dusting, such as wiping the surface. Since THC is assumed to be degraded from upward-facing organic films through heterogeneous ozonolysis with a rate constant on the order of magnitude of 10^{-5} s^{-1} (see Table S4†), surface cleaning has no significant impact unless it is practiced daily or more frequently. Here, we consider cleaning scenarios with a frequency of once per day and efficiencies ranging from 20% to 80%.

Sensitivity analysis

The predictions of this study are based on several fixed input parameters, even though in reality their values will vary, i.e., these inputs are both variable and uncertain. Variability applies to parameters that can be characterized experimentally with high precision but may vary from one case to another. The air exchange rate, PM concentration in indoor air, and the frequency of touching indoor surfaces, among others, are examples of input parameter mostly subject to variability. On the other hand, uncertainty refers to parameters whose experimental determination may incur significant error. Air-to-surface partitioning ratios and the parameters describing the kinetics of THC surface chemistry are the input parameters most affected by uncertainty.

A sensitivity analysis was performed to assess the effect of parameter variability or uncertainty on the average body mass-normalized uptake rate. To identify parameters which have the greatest impact on the model output, first, the effect of perturbing the input value by 10% was evaluated, as shown by eqn (7).

$$S = \frac{|\text{Exp}_{\text{avg}}(1.1X_0) - \text{Exp}_{\text{avg}}(0.9X_0)| / \text{Exp}_{\text{avg}}(X_0)}{(1.1X_0 - 0.9X_0)/X_0} \\ = 5 \times \frac{|\text{Exp}_{\text{avg}}(1.1X_0) - \text{Exp}_{\text{avg}}(0.9X_0)|}{\text{Exp}_{\text{avg}}(X_0)} \quad (7)$$

In eqn (7), X_0 is the default value for a given input parameter. S in eqn (7) is equivalent to the nondimensionalized value of the slope of the line passing through two points corresponding to model outputs calculated by varying the input parameter X_0 by 10%. $S = 0$ signifies no sensitivity of the model output to the parameter of interest over a 10% variability interval. On the other hand, the more S deviates from zero, the more sensitive the model output is to X_0 . We assumed any S value higher than or equal to 0.01 to signify an influential input parameter.

The variability of input parameters selected per the above criterion was considered in a Monte Carlo simulation. More details on the sensitivity analysis and the Monte Carlo simulation are discussed in Section S4.† Briefly, the model output is evaluated for several scenarios, each comprising a combination of the selected parameters sampled from distributions suggested in the scientific literature.

Results and discussion

Indoor fate of THC emitted from cannabis smoking

Fig. 1(a) shows the evolution of monthly-averaged concentrations of THC within different indoor compartments resulting from periodic cannabis smoking discussed in the Methods section. THC compartmental concentrations tend to peak during smoking time and decay afterwards, as discussed in the next paragraphs. Thus, the concentrations depicted in Fig. 1(a) are dominated by lower values associated with longer non-smoking times. Due to the high affinity of THC to organic matrices, THC distribution between indoor compartments is highly uneven making the concentration profiles in Fig. 1(a) vary across several orders of magnitude. THC monthly averaged



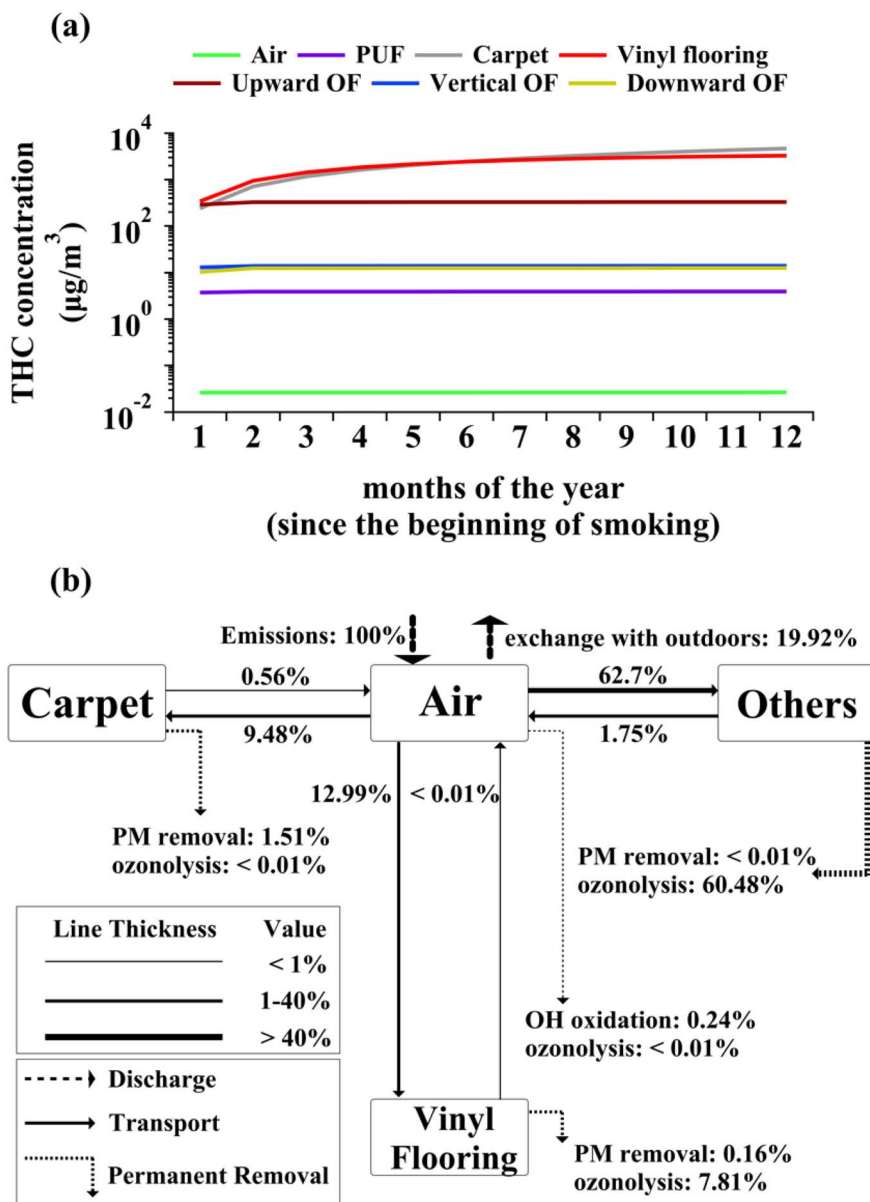


Fig. 1 Indoor fate of THC emitted by cannabis smoking. (a) THC concentration ($\mu\text{g m}^{-3}$) over the first year since the beginning of periodical cannabis smoking in the evaluative indoor environment, (b) schematic diagram showing the network of indoor compartments and average THC mass exchange/loss rates as percentages relative to the total THC released into the evaluative indoor environment. Arrow thicknesses in panel (b) are proportional to exchange/loss rates. "Others" refers to PUF and surface organic films.

concentrations do not vary by more than 1% beyond the first six months for all compartments other than carpet and vinyl flooring. THC concentrations in carpet and vinyl flooring continue to increase slowly beyond the first twelve months since daily cannabis smoking commenced. Thus, a steady-state analysis is appropriate if one is interested in long-term THC concentrations from cannabis smoking in indoor air and non-flooring and paving surface compartments.

THC concentration in each indoor compartment depends on the respective input and output mass transfer fluxes. The diagram in Fig. 1(b) shows the network of indoor compartments and the average THC mass transfer rates. Since Fig. 1(a) shows

that THC concentrations remain almost invariant in surface compartments other than carpet and vinyl flooring, all compartments other than those two are grouped into "Others" in Fig. 1(b). Mass transfer and loss rates scale with the release rate due to linearity of the mass balance equations.²³ Hence, the transfer and loss rates are expressed as percentages relative to the THC emission rate in Fig. 1(b). Note that the ozonolysis processes shown in Fig. 1(b) are associated with the bulk phase of each compartment (*e.g.*, carpet fibers and pad), not the accumulated PM.

More than 99% of airborne THC readily partitions to particulate matter (PM) given its low volatility (see Table S2†).



Consequently, particle deposition is the dominant mechanism for THC transfer from air to indoor surfaces. Fig. 1(b) indicates that THC transport to the outdoors due to ventilation is smaller than THC exchange with indoor compartments. The reduced rates of particulate deposition onto vertical and horizontal downward-facing surfaces lead to smaller THC concentrations associated with such surfaces compared to those in horizontal upward-facing ones. Although THC input mass transfer rate is the highest for upward-facing organic films, the rapid heterogeneous ozonolysis prevents accumulation in these films. The higher THC concentrations in carpet result from slow removal by dusting and heterogeneous ozonolysis on fibrous surfaces. Although ozonolysis kinetics are similar between vinyl flooring and upward-facing organic films (see Table S4[†]), THC reactive loss is faster for the latter given its higher surface-to-volume ratio. THC concentrations in PUF are comparable with those in non-upward-facing organic films. This trend mainly stems from the low surface area of PUF compared to other compartments, which reduces its capacity for deposition of THC through PM. As evident from Fig. 1(b), reactive loss of THC in the gas phase due to oxidation by indoor ozone and hydroxyl radicals is not significant for airborne THC. Note that this study does not consider THC heterogeneous ozonolysis on PM.

THC concentrations are expected to be highly dynamic around the smoking periods. Inspecting compartmental concentration evolution provides insights into the role of various compartments as effective THC reservoirs. To ensure that the transient effects associated with early months of cannabis smoking do not affect this analysis, we examined THC concentrations during and after the last smoking period within

the one-year time domain of the model. Fig. 2(a) shows THC enhancements in each indoor compartment during the last smoking period. The airborne concentration increases sharply for about fifty seconds before PM deposition commences to prevent further increase. Surface compartments start to have higher THC concentrations with a delay of about 10 minutes. This lag is comparable to rate of deposition of PM₁₀.¹⁶ Moreover, the timescale associated with THC diffusion to surfaces is about 12 minutes based on THC diffusion coefficient calculated following Li *et al.*¹⁸ and assuming the mass transfer boundary layer thickness above indoor surfaces to be 5 millimetres. Therefore, THC concentration increases even more during the last fifty minutes of smoking due to the synergistic effect of PM deposition and direct partitioning from the gas phase. Note that the rate of THC concentration increase is comparable between vinyl flooring and carpet, but upward-facing organic films have a more intense increase in THC content mainly because of the higher partitioning coefficient of THC from air to organic films (see Section S2[†]). Fig. 2(a) shows that vertical and downward-facing organic films begin with comparable THC concentrations; however, the rate of accumulation on downward-facing surfaces ends up being lower than on vertical films owing to negligible PM deposition rates. Fig. 2(b) demonstrates THC decay in each compartment during the 23 hour period following cannabis smoking. Continuous PM deposition causes airborne concentrations to decrease rapidly within about thirty seconds after smoking. Fig. 2(b) shows that during the first four hours after smoking, THC concentrations on surface compartments do not vary appreciably as a result of continuous deposition and partitioning. THC decays with a relatively uniform rate from

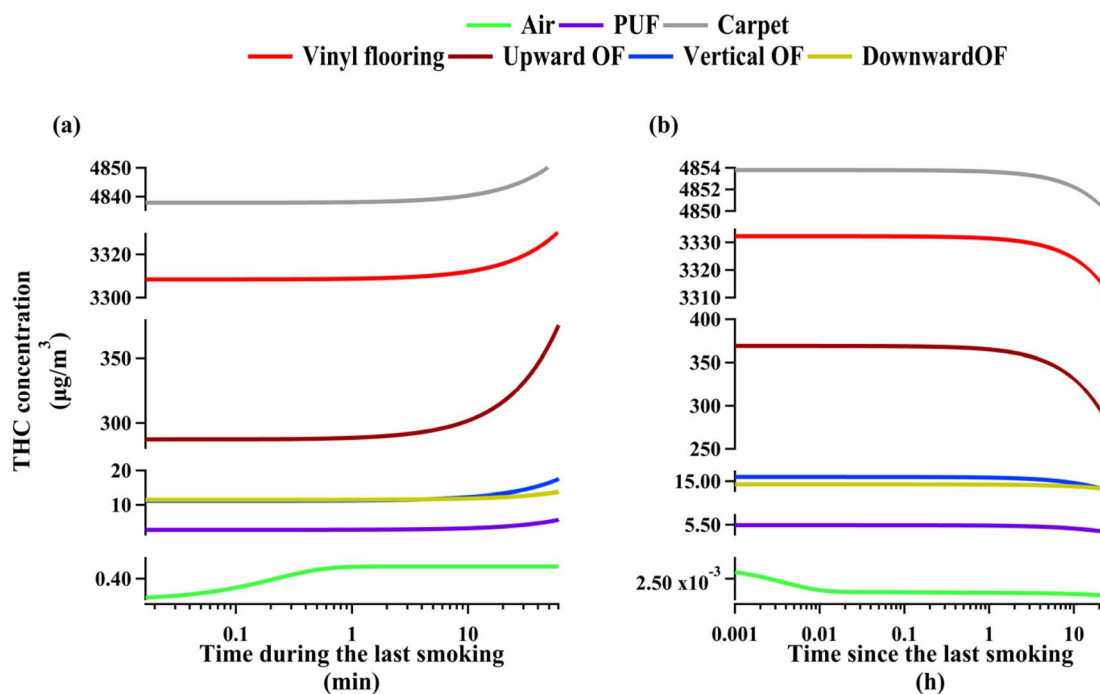


Fig. 2 THC compartmental concentration evolution during (a) the last cannabis smoking period, (b) the 24 hour interval following the last cannabis smoking.



surface compartments other than carpet, vinyl flooring, and upward-facing organic films between the first and fourth hours after smoking. The decay of THC from the three compartments mentioned above is more intensified as a result of higher dusting rate for carpets and quite rapid heterogeneous ozonolysis on vinyl flooring and upward-facing organic films beyond the first four hours. See Section S3.4† for more information on crucial processes affecting THC decay from indoor surfaces during non-smoking periods.

Evaluating model predictions against experimental data on indoor air THC concentrations from cannabis smoking

The scientific literature is relatively sparse regarding experimental studies targeting air concentration of THC from cannabis smoking. Some studies have reported time-independent THC air concentrations. Yeh *et al.* thoroughly reviewed experimental data on THC concentrations in indoor air,¹⁴ with two studies reporting temporal variations of THC concentrations in controlled indoor spaces following cannabis smoking. Niedbala *et al.*²⁴ measured air concentrations of cannabis in a closed room with no ventilation with a volume of 36 m³ (3 m × 4 m × 3 m) for 170 minutes. A cannabis cigarette containing ~13 mg of THC was smoked during the first 20 minutes. We assumed the whole floor area was covered by vinyl flooring. No carpet and PUF compartments were considered. We assumed the area of upward-facing organic films to be 50% of the total floor area. The area of the vertical organic films and downward-facing organic films were assumed to be equal to the total wall area and ceiling area, respectively. THC concentrations predicted with our model during and after smoking are in fair agreement with the experimental data by Niedbala *et al.*²⁴ (Fig. 3(a)). The middle data point is associated with an interval starting immediately after smoking and ending about 10 minutes later. The model predicts that THC concentration in air plunges by about two orders of magnitude during this interval. The measured data are within 20% of the average THC air concentration estimated by the model during the measurement interval.

Cone *et al.* measured THC concentration in air during a one-hour experiment in a controlled indoor space.²⁵ During different experiments either two or eight cannabis cigarettes containing ~25 mg THC were smoked during the first and third quarters of the measurement interval. We again assumed the whole floor area to be covered by vinyl flooring. The dimensions of other surface compartments were adjusted as described above for Niedbala *et al.*²⁴ We only considered data with no ventilation (*i.e.*, closed door) since the air exchange rate was not reported for the case of open doors. Our predictions agree with the measurements by Cone *et al.*²⁵ within 2 to 30% for data points associated with the end of smoking intervals (Fig. 3(b)). However, the model predicts a much sharper decrease in concentration during non-smoking intervals compared to the measured data. Since we identified PM deposition as the dominant process affecting THC air concentrations (see Table S8†), the evaluative environment studied by Cone *et al.*²⁵ might have PM with lower deposition rates leading to a less

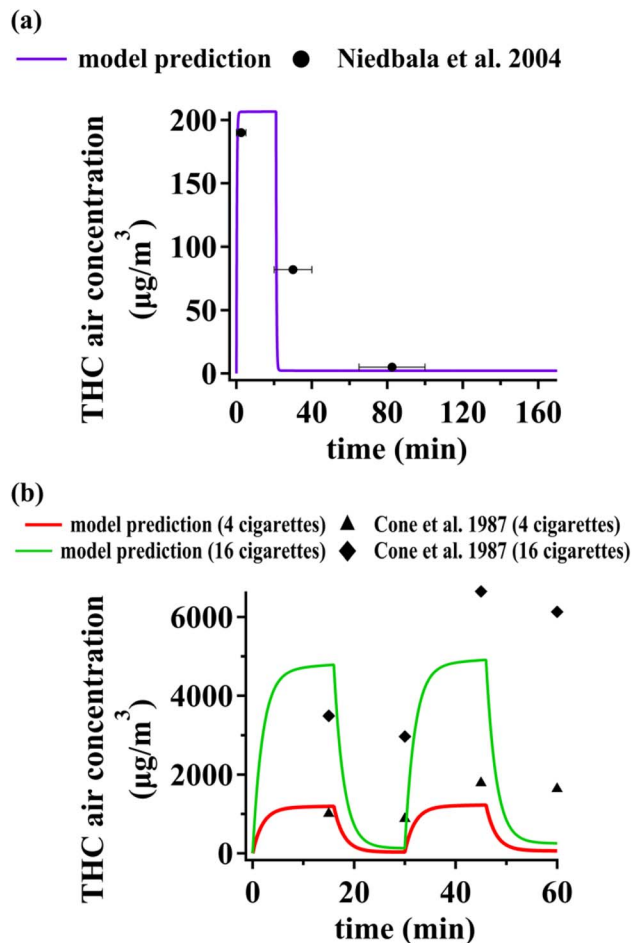


Fig. 3 Comparison of model predictions for THC concentration in indoor air against data reported by (a) Niedbala *et al.*,²⁴ (b) Cone *et al.*²⁵

pronounced THC concentration decrease during non-smoking periods. Furthermore, measurement timing may have deviated from the very moments of transitioning from a smoking interval to a non-smoking one. Fig. S1(b)† shows that if one allows for 5 minutes of uncertainty for concentration measurements at $t = 30$ min and $t = 60$ min, model predictions would be within 35% of measurements.

Overall, considering the high temporal variability of THC concentrations during smoking, experimental studies recording concentration at high time resolution should be contemplated. Online measurement techniques may be more appropriate compared to off-line methods for this purpose.

Note that the numerical value of THC concentrations in indoor air measured by Niedbala *et al.*²⁴ and Cone *et al.*²⁵ differ remarkably from the ones we calculate for our original evaluative exposure scenario, displayed in Fig. 1 and 2. This is not only because of the widely different experimental conditions (*e.g.* more intense THC emissions, smaller indoor space volume, and zero air exchange rate), but also because the levels in Fig. 1 and 2 reflect long term averages over periods that include long periods of non-smoking, when air concentrations are much lower.



Involuntary exposure of indoor residents to THC from cannabis smoking

Fig. 4 shows average body mass-normalized daily THC uptake for an adult person (Fig. 4(a)) and a toddler (Fig. 4(b)). Each exposure result shown in Fig. 4 is the result of averaging uptake rates of THC over the applicable time interval. Accordingly, the uptake rates were averaged over one-hour smoking periods and the whole one-year period for second-hand and total uptake, respectively. The third-hand uptake rates were averaged over a reduced one-year period resulting from eliminating the smoking hours. As a result of this difference in averaging times, the total uptake values in Fig. 4 are not necessarily equal to the sum of second- and third-hand uptakes. Note that the uptake rates depend on body size. For instance, people with larger lung volumes are more exposed to air pollutants through inhalation. Therefore, the uptake rates shown in Fig. 4 are normalized based on body weight.

Given the uncertainty in THC bioavailability, the uptake values of Fig. 4 must only be interpreted in the context of THC bioavailability values as discussed in Section S3.3.† The intake rates (*i.e.*, exposure rates without accounting for bioavailability) serve as upper limits for passive exposure rates to THC. Fig. 4 shows that THC body mass-normalized uptake rates for toddlers are one to two orders of magnitude higher than for adults. The temporarily high THC concentrations during smoking periods caused second-hand exposure to be remarkably more intense than third-hand exposure. In fact, third-hand exposure is negligible for adults. Our analysis shows that THC body concentrations can momentarily exceed the threshold of 5 ng ml⁻¹ per Canadian Drug-impaired Driving Laws²⁶ due to second-hand smoking effects for both adults and toddlers. Toddler's third-hand exposure is high enough to lead to body concentration exceeding the criterion mentioned above by more than five-fold. Overall, we assess passive exposure to THC to be critical for residents of all ages per the smoking settings assumed in this study. Less frequent cannabis smoking or smoking cigarettes with less THC content can lead to lower uptake rates.

Fig. 4(a) shows that for adults, inhalation is the primary route of exposure to THC from cannabis smoking emissions, while dermal permeation and non-dietary ingestion make a negligible contribution. This trend is valid for both second- and third-hand exposure. Adults are assumed to touch indoor surfaces less frequently, especially floor coverings, and engage in much less hand to mouth contact than toddlers. For toddlers, on the other hand, non-dietary ingestion mediated by hand to mouth contact or object mouthing is predicted to be the main route of exposure to THC except during smoking time when airborne concentrations are high. Our model predicts the THC concentration to be higher on upward-facing organic films, which are approximately equivalent with indoor objects that toddlers mouth, compared to hand surfaces. This difference leads to object mouthing to account for more than 98% of toddler's non-dietary ingestion. Note that this result indicates that toddler's THC uptake reduces appreciably when the objects in the smoking site are not prone to toddler mouthing.

Dermal permeation's share in THC uptake is estimated to be negligible for both toddlers and adults. Human skin surface area is not sufficiently high for THC deposition rates from air to be significant, even if the total skin area is assumed to be exposed. Skin contact with other objects often occurs over short intervals so that the THC transfer to the skin is limited. As discussed in Section S3,† THC is relatively lipophilic and diffuses slowly through skin layers after adhering to the skin, which delays THC entrance into the systemic blood cycle.

Strategies to mitigate indoor occupants' exposure to THC from cannabis smoking

Ventilation intensity is often expressed through the air exchange rate, defined as the ratio of volumetric rate of air transport out of the indoor space to the space volume. Fig. 5(a) shows how enhancing the air exchange rate reduces average annual body mass-normalized THC uptake following one year of periodic cannabis smoking, as discussed in the Methods section. Fig. 5(a) starts from an air exchange rate of 1.00 h⁻¹, which is about 30% higher than the base case scenario with a ventilation rate of 0.75 h⁻¹, and examines the effect of ventilation enhancement for values up to 2.0 h⁻¹. Ventilation enhancement during smoking is predicted to reduce adult and toddler THC uptake rates by about 65% and 70%, respectively. Mitigation of the toddler exposure is due to reduced THC concentration on indoor surfaces, which affects exposure through non-dietary ingestion. On the other hand, increased ventilation after smoking reduces adult's THC uptake by less than 2% whereas it can decrease toddler's THC uptake by about 50%. This divergence occurs because post-smoking exposure to THC (*i.e.*, third-hand smoking) is negligible for adults, contrary to the toddlers' case (see Fig. 4).

Clean Air Delivery Rate (CADR) is a good indicator of PM removal efficacy as it accounts for both air handling rate and PM removal efficiency (see Table S4†). Fig. 5(b) shows the reduction in average annual body mass-normalized THC uptake by indoor residents due to equipping the space with a PM-removing device. PM removal associated with a CADR of 500 m³ h⁻¹ can reduce adult's and toddler's THC uptake by 78% and 83%, respectively. This CADR is equivalent to a handling capacity of 1000 m³ h⁻¹ assuming PM efficiency to be about 50%. The air exchange rate rarely exceeds 2 h⁻¹²⁵, which corresponds to a volumetric air exchange rate of 150 m³ h⁻¹ for the evaluative environment of interest in this study. Given that commercial air cleaners can have CADRs as high as 500 m³ h⁻¹,²⁷ especially when they are newly installed with clean filters, they can have THC removal capacities which are not achievable by enhanced ventilation. As expected, based on discussions above, PM removal after smoking has no significant effect on adult's THC uptake but can reduce toddler's THC uptake by about 52% when CADR is 500 m³ h⁻¹. Note that contrary to a relatively uniform decrease of THC uptake with increasing CADR for adults, there is a sharper decrease for toddlers from CADR = 200 m³ h⁻¹ to CADR = 300 m³ h⁻¹. This is because beyond CADR values of about 230 m³ h⁻¹ direct THC transfer from gas phase to organic films exceeds PM-mediated transfer.



Accounting for spatial variability of indoor PM concentrations is beyond the scope of this work. Considering that we assumed the indoor space to be well-mixed, PM removal can be an even more reliable mitigation strategy to address involuntary exposure to THC if cannabis smoking is done near the air cleaner device. Similarly, placing the air cleaner at zones far from the cannabis smoking point may result in uptake reductions much lower than the values suggested by this study.

Fig. 5(c) depicts average annual body mass-normalized THC uptake when indoor dwellers leave the space for six-hour intervals. The scenarios are categorized based on the time gap between the end of indoor absence and the beginning of cannabis smoking. Therefore, given that we consider one hour of cannabis smoking per day, the first category in Fig. 5(c) corresponds to the case where the resident enters the room just after smoking has ceased. An adult's THC uptake falls by more than 95% for all cases of overlap between the absence interval and the smoking period (Fig. 5(c)). Since a remarkable fraction of toddler's THC uptake is associated with third-hand smoking effects, leaving the space during cannabis smoking is not as effective. Six hours of absence comprising the smoking period can reduce a toddler's exposure to THC by about 50%. Among

the first six categories of absence scenarios, there is no remarkable difference in THC uptake for both adults and toddlers, which indicates that the one-hour absence from the space during smoking is the primary contributor to exposure mitigation from leaving the site. The last category in Fig. 5(c) corresponds to being present during cannabis smoking and leaving the space immediately afterwards. This scenario leads to no significant reduction to adult's THC uptake but can still reduce the toddler's uptake by about 20% because leaving the space, irrespective of its timing, removes a fraction of third-hand exposure for toddlers.

Fig. 5(d) shows how surface cleaning affect average annual body mass-normalized THC uptake of passive indoor residents. Given the negligible contribution of surface-mediated non-dietary ingestion to adult's exposure to THC, surface cleaning leads to no significant impact on adult's exposure to indoor THC. On the other hand, the scenario associated with 80% cleaning efficiency can reduce toddler's THC uptake by about 20% through targeting object mouthing-mediated non-dietary ingestion. Surface cleaning cannot reduce the toddler's THC uptake by more than 50% unless cleaning frequency is increased beyond once per every ten hours (data not shown).

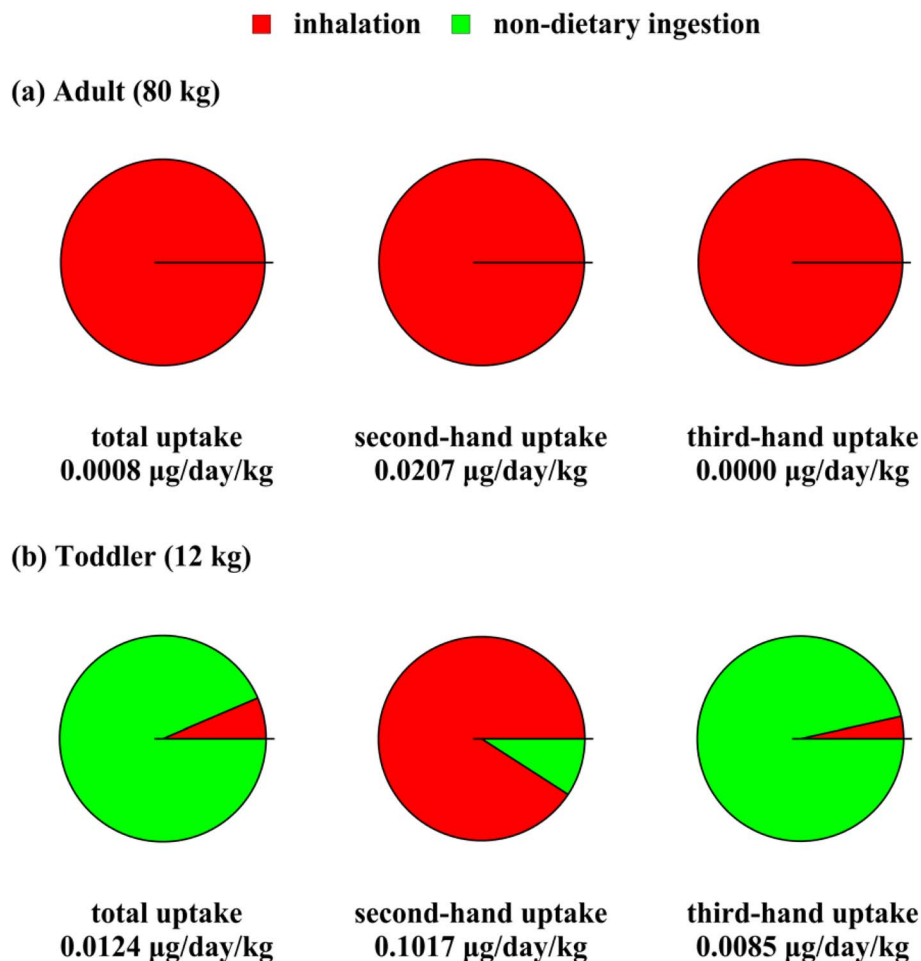


Fig. 4 Average body mass-normalized THC uptake rate from cannabis smoking via different routes, for (a) adults and (b) toddlers, as second-hand, third-hand, and total exposure.



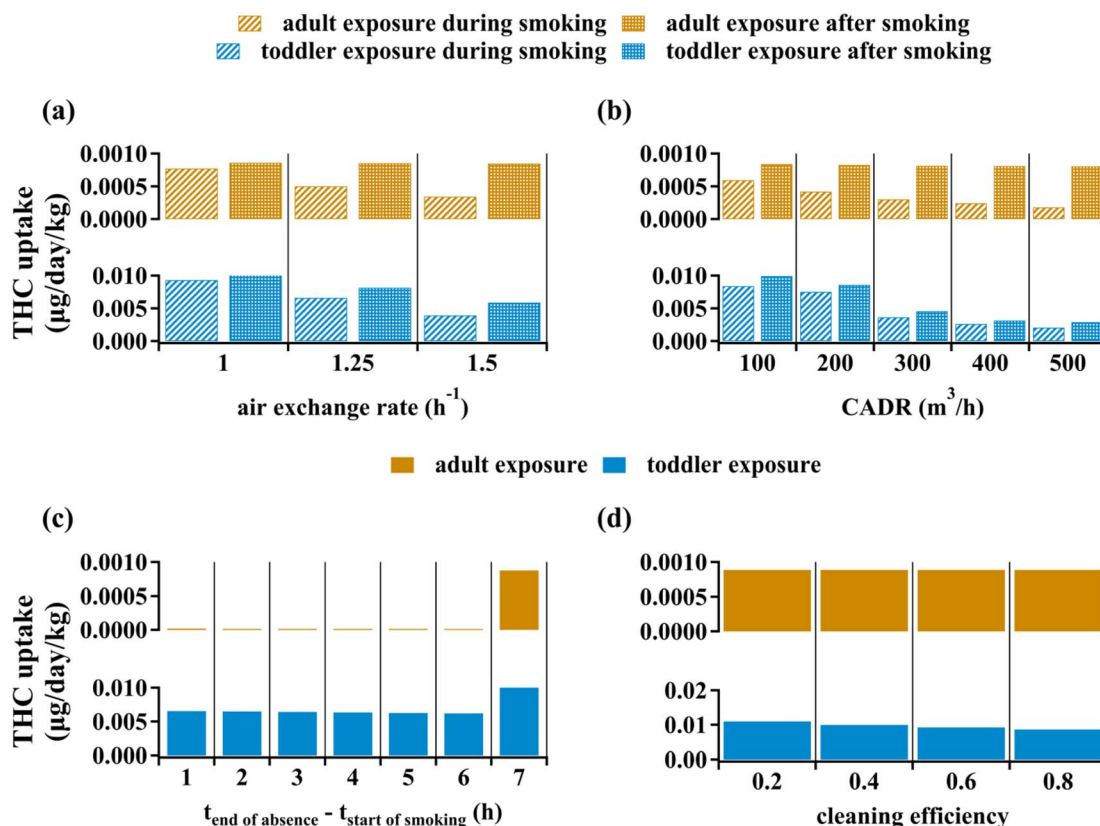


Fig. 5 Mitigation of indoor occupants' exposure to THC by (a) enhancing air exchange rate, (b) reducing PM concentrations, (c) letting passive indoor residents leave the indoor space for six-hour intervals, and (d) THC cleaning from upward-facing organic films. All body-mass normalized uptake values are averaged over one year of periodic cannabis smoking considering the passive indoor occupants to be an adult (80 kg) and a toddler (12 kg).

Sensitivity analysis

The model performance depends on the accuracy of input parameters, and many of these parameters can vary from one exposure scenario to another. As discussed in Section S4 of the ESI,[†] the exposure predictions for both adults and toddlers are appreciably affected by the variability in the PM deposition and resuspension rates, the dust removal rate, indoor space size, inhalation and object mouthing frequency, and the air exchange rate variability. Additionally, uncertainty in THC vapor pressure and octanol-air partitioning coefficient have a profound influence on the model outputs. Fig. 6 depicts the results of Monte Carlo simulations performed as described in the Methods section and Section S4[†] along with uptake predictions based on default input parameters (also shown in Fig. 4). The medians of THC uptakes for alternative scenarios associated with parameter variability differ from the default scenario by less than 10% for both adults and toddlers. Scenarios associated with reduced particle deposition rates and smaller indoor sizes lead to higher airborne THC concentrations which can lead to adult uptakes about two times higher than the default prediction. Since finer airborne particles have smaller deposition rates,¹⁷ indoor spaces with PM size distribution skewed towards smaller particles can lead to adult uptakes much higher than our prediction. On the other hand,

a combination of higher deposition rates and lower dusting rates can lead to toddler THC uptakes of about 90% higher than the default case due to enhanced THC surface concentrations. Note that enhanced deposition rates lead to reduced inhalation and increased non-dietary ingestion exposure. Since the latter is more crucial in a toddler's THC uptake, the net effect is an increase in total involuntary exposure to THC for younger residents.

THC liquid vapor pressure, P_L , and octanol-air partitioning coefficient, K_{OA} , were identified as parameters whose uncertainty impacts model outputs significantly (see Section S4[†]). Since P_L and K_{OA} cannot vary independently (see Section S2[†]), we only allowed for the former's variation and the latter was calculated accordingly (see Section S4[†]). Parameter uncertainty leads to alternative predictions for adult THC uptake which deviate by less than 1% from default model output (Fig. 6(a)). On the other hand, the median of the toddler's THC uptake associated with alternative scenarios of parameter uncertainty is 30% higher than the default model output. In extreme cases, such scenarios can lead to toddler THC uptakes which are more than thirty times higher than the default (Fig. 6(b)). These cases arise from an enhanced octanol-air partition ratio and reduced liquid vapor pressure which lead to more THC partitioning from air to indoor surfaces affecting non-dietary ingestion.



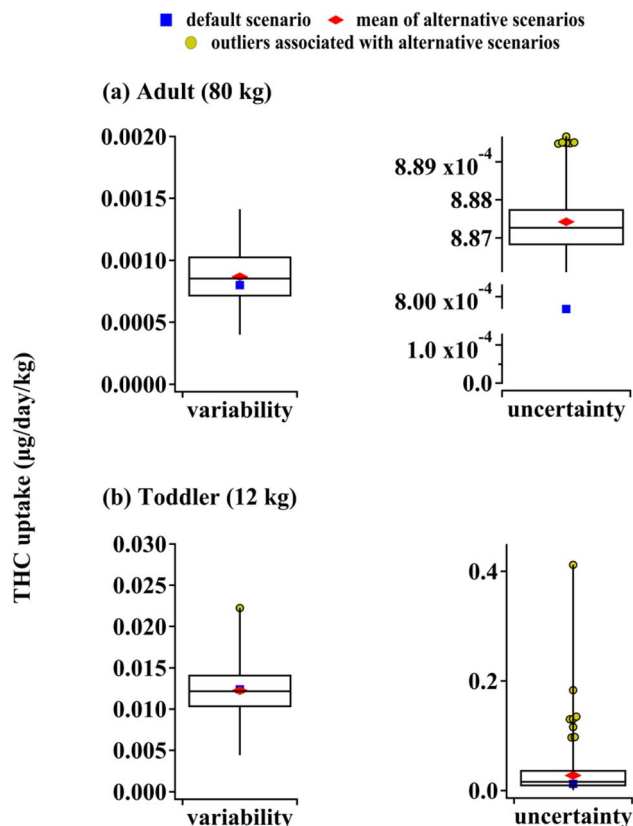


Fig. 6 Monte Carlo simulation of the sensitivity of the estimated annual average body-mass normalized THC uptake rates for adults (a) and toddlers (b) to uncertainty and variability of input parameters along with the results for the default scenario (blue square). Box plot whiskers correspond to minimum and maximum of individual scenario results. The outliers exceed the third quartile by at least 1.5 times of the interquartile range.

Conclusion and implications

A level IV fugacity model was used in this work to characterize mass transfer phenomena affecting the indoor fate of THC emissions from indoor cannabis smoking. Carpet and flooring materials were found to be significant reservoirs for indoor THC. The exposure analysis was performed for indoor occupants stratified into adults and toddlers as broad groups distinguished by their hygienic habits and physiological properties. Second-hand involuntary THC uptakes by residents of all ages were high enough to lead to THC body concentrations temporarily exceeding the thresholds associated with Canadian Federal laws of drug-impaired driving. Toddlers' estimated exposure to THC, dominated by non-dietary ingestion, was higher than adults by orders of magnitude. Toddlers' exposure to THC was mainly mediated by object mouthing. These results underscore the importance of preventing infants from accessing spaces where cannabis smoking takes place, even during periods when there is no smoking activity.

The usefulness of a few measures to mitigate exposure to THC was discussed. Strategies aimed at cleansing indoor air,

either as a whole or only its PM component, can lead to substantial exposure reductions for both adults and toddlers. THC accumulation is limited in indoor spaces with good ventilation equipped with PM filtration devices. Employing enhanced ventilation, however, begs the question of the location to which air is exchanged. Any ventilation scheme that includes purging the air from the smoking site to other indoor spaces may address the exposure issue within the space of interest at the expense of putting other indoor locations at risk. Leaving the space during smoking can significantly reduce adult exposure but is less effective in reducing THC uptake of toddlers (only about 20%). Surface cleaning can reduce toddlers' exposure to THC only when its effectiveness in removing THC is comparable to fast surface reactions. Discussing the feasibility of such cleaning measures and their potential side effects is beyond the scope of this study.

This model can be applied to conditions different from those used here (see Section S5†). For example, the occurrence and relative size of compartments or the air exchange rate varies widely between a room within a residence, a smoking space in a club, or a motor vehicle (for instance, see Niedbala *et al.*).²⁸ Emission rates and patterns often will deviate from what was assumed here. The model parameters can be tailored to yield insights on temporal indoor fate of, and exposure to, cannabis emissions in the absence of measurements.

A sensitivity analysis identified parameters with a large impact on model predictions. Uncertainty in THC partitioning ratios cause variations in the exposure estimated for the toddler by multiple orders of magnitude. We suggest that future environmental chamber studies investigating THC partitioning to, and chemistry on, typical indoor articles could reduce parameter uncertainty by suggesting bounding values associated with extreme conditions.

The modeling framework used in this study is subject to some limitations. We did not consider spatial variations in THC concentrations, since we assume the indoor evaluative environment to behave like a well-mixed chamber. This approach can therefore not serve to inspect phenomena related to specific locations²⁹ such as applying enhanced ventilation or PM filtration in the vicinity of the smoking site. We assumed THC to be in thermodynamic equilibrium between the bulk phase and the accumulated PM in each indoor compartment, which may not always be the case.³⁰ Several behavioral phenomena (*e.g.*, handwashing and surface handling) were treated as occurring constantly at average rates instead of treating them as processes that intermittently occur similar to the approach utilized by Julian *et al.*³¹ This approximation may lead to inaccurate instantaneous intake rates if one tries to examine exposure to THC with greater time resolution than what is discussed above. Some of the variables considered for sensitivity analysis within the Monte Carlo simulation may not change independently from each other. For instance, depending on the configuration of indoor objects, there might be scenarios where an increase in upward-facing organic film occurs accompanied by a decrease in exposed floor, hence reducing the surface area attributed to vinyl flooring or carpet.



Author's contributions

Amirashkan Askari conducted the formal analysis and wrote the original draft. Frank Wania contributed through conceptualization, validation, reviewing, and editing the paper text. Arthur Chan supervised the study and helped with conceptualization, validation, reviewing, and editing the paper text.

Conflicts of interest

All authors declare that they have no conflicts of interest.

Acknowledgements

The authors acknowledge Sivani Baskaran for performing THC thermodynamic equilibrium calculations using the COSMOtherm software. We also acknowledge Professor Jonathan Abbatt for providing kinetic parameters of THC heterogeneous ozonolysis. We acknowledge the support of the Natural Sciences and Engineering Research Council of Canada (NSERC) Discovery Grant (RGPIN-2019-06936).

References

- 1 WHO, *Alcohol, drugs and addictive behaviours (ADA)*, [https://www.who.int/teams/mental-health-and-substance-use/alcohol-drugs-and-addictive-behaviours/drugs-\(psychoactive\)/cannabis](https://www.who.int/teams/mental-health-and-substance-use/alcohol-drugs-and-addictive-behaviours/drugs-(psychoactive)/cannabis), accessed 12 November 2020.
- 2 *Annual prevalence of the use of drugs by region and globally*, https://dataunodc.un.org/drugs/prevalence_regional, accessed 12 November 2020.
- 3 Health Canada, *Canadian Cannabis Survey 2019 – Summary*, <https://www.canada.ca/en/health-canada/services/publications/drugs-health-products/canadian-cannabis-survey-2019-summary.html>, accessed 12 November 2020.
- 4 *Canadian Cannabis Survey 2021: Summary*, 2021.
- 5 A. Posis, J. Bellettiere, S. Liles, J. Alcaraz, B. Nguyen, V. Berardi, N. E. Klepeis, S. C. Hughes, T. Wu and M. F. Hovell, Indoor cannabis smoke and children's health, *Prev. Med. Rep.*, 2019, **14**, 100853.
- 6 J. Siegel, IAQ implications of cannabis legalization, *ASHRAE J.*, 2017, **59**, 62–64.
- 7 I. Amirav, A. Luder, Y. Viner and M. Finkel, Decriminalization of Cannabis – potential risks for children?, *Acta Paediatr.*, 2011, **100**, 618–619.
- 8 R. D. Goodwin, C. P. Keely, S. Santoscoy, N. Bakoyiannis, D. S. Hasin, B. N. Collins, S. J. Lepore and M. M. Wall, Trends in cannabis and cigarette use among parents with children at home: 2002 to 2015, *Pediatrics*, 2018, **141**(6), e20173506.
- 9 K. S. Grant, R. Petroff, N. Isoherranen, N. Stella and T. M. Burbacher, Cannabis use during pregnancy: pharmacokinetics and effects on child development, *Pharmacol. Ther.*, 2018, **182**, 133–151.
- 10 F. Degenhardt, F. Stehle and O. Kayser, *Handbook of Cannabis and Related Pathologies: Biology, Pharmacology, Diagnosis, and Treatment*, Elsevier Inc., 2017, pp. 13–23.
- 11 B. Nie, J. Henion and I. Ryona, The Role of Mass Spectrometry in the Cannabis Industry, *J. Am. Soc. Mass Spectrom.*, 2019, **30**, 719–730.
- 12 S. L. Chou, Y. C. Ling, M. H. Yang and C. Y. Pai, Determination of Δ^9 -tetrahydrocannabinol in indoor air as an indicator of marijuana cigarette smoking using adsorbent sampling and in-injector thermal desorption gas chromatography-mass spectrometry, *Anal. Chim. Acta*, 2007, **598**, 103–109.
- 13 A. Cecinato, P. Romagnoli, M. Perilli and C. Balducci, Psychotropic substances in house dusts: a preliminary assessment, *Environ. Sci. Pollut. Res.*, 2017, **24**, 21256–21261.
- 14 K. Yeh, L. Li, F. Wania and J. P. D. Abbatt, Thirdhand smoke from tobacco, e-cigarettes, cannabis, methamphetamine and cocaine: partitioning, reactive fate, and human exposure in indoor environments, *Environ. Int.*, 2022, **160**, 107063.
- 15 C. J. Weschler and W. W. Nazaroff, Growth of organic films on indoor surfaces, *Indoor Air*, 2017, **27**, 1101–1112.
- 16 X. Zhang, J. A. Arnot and F. Wania, Model for screening-level assessment of near-field human exposure to neutral organic chemicals released indoors, *Environ. Sci. Technol.*, 2014, **48**, 12312–12319.
- 17 H. M. Shin, T. E. McKone, N. S. Tulve, M. S. Clifton and D. H. Bennett, Indoor residence times of semivolatile organic compounds: model estimation and field evaluation, *Environ. Sci. Technol.*, 2013, **47**, 859–867.
- 18 L. Li, J. A. Arnot and F. Wania, Towards a systematic understanding of the dynamic fate of polychlorinated biphenyls in indoor, urban and rural environments, *Environ. Int.*, 2018, **117**, 57–68.
- 19 D. Mackay, *Multimedia Environmental Models : the Fugacity Approach*, Taylor and Francis, 2nd edn, 2001.
- 20 J. M. Prausnitz, R. N. Lichtenthaler and E. G. de Azevedo, *Molecular Thermodynamics of Fluid-phase Equilibria*, Pearson Education, 3rd edn, 1998.
- 21 W. R. Ott, T. Zhao, K. C. Cheng, L. A. Wallace and L. M. Hildemann, Measuring indoor fine particle concentrations, emission rates, and decay rates from cannabis use in a residence, *Atmos. Environ.: X*, 2021, **10**, 100106.
- 22 A. Berthet, M. de Cesare, B. Favrat, F. Sporkert, M. Augsburg, A. Thomas and C. Giroud, A systematic review of passive exposure to cannabis, *Forensic Sci. Int.*, 2016, **269**, 97–112.
- 23 W. Stiver and D. Mackay, The linear additivity principle in environmental modelling: application to chemical behaviour in soil, *Chemosphere*, 1989, **19**, 1187–1198.
- 24 S. Niedbala, K. Kardos, S. Salamone, D. Fritch, M. Bronsgeest and E. J. Cone, Passive Cannabis Smoke Exposure and Oral Fluid Testing, *J. Anal. Toxicol.*, 2004, **28**, 546–552.
- 25 E. J. Cone, R. E. Johnson, W. D. Darwin, D. Yousefnejad, L. D. Mell, B. D. Paul and J. Mitchell, Passive Inhalation of Marijuana Smoke: Urinalysis and Room Air Levels of Δ^9 -Tetrahydrocannabinol, *J. Anal. Toxicol.*, 1987, **11**, 89–96.



- 26 *Frequently Asked Questions – Drug-Impaired Driving Laws*, <https://www.justice.gc.ca/eng/cj-jp/sidl-rlcfa/qa2-qr2.html>, accessed 11 November 2022.
- 27 K. C. Noh and M. Oh, Variation of clean air delivery rate and effective air cleaning ratio of room air cleaning devices, *Build. Environ.*, 2015, **84**, 44–49.
- 28 R. S. Niedbala, K. W. Kardos, D. F. Fritch, K. P. Kunsman, K. A. Blum, G. A. Newland, J. Waga, L. Kurtz, M. Bronsgeest and E. J. Cone, Passive Cannabis Smoke Exposure and Oral Fluid Testing. II. Two Studies of Extreme Cannabis Smoke Exposure in a Motor Vehicle, *J. Anal. Toxicol.*, 2005, **29**, 607–615.
- 29 E. Wigzell, M. Kendall and M. J. Nieuwenhuijsen, The spatial and temporal variation of particulate matter within the home, *J. Exposure Anal. Environ. Epidemiol.*, 2000, **10**, 307–314.
- 30 J. Cao, J. Mo, Z. Sun and Y. Zhang, Indoor particle age, a new concept for improving the accuracy of estimating indoor airborne SVOC concentrations, and applications, *Build. Environ.*, 2018, **136**, 88–97.
- 31 T. R. Julian, R. A. Canales, J. O. Leckie and A. B. Boehm, A Model of Exposure to Rotavirus from Nondietary Ingestion Iterated by Simulated Intermittent Contacts, *Risk Anal.*, 2009, **25**(5), 617–632.

